

## IMMOBILIZING MICROALGAE IN HYBRID MATRICES AS A GREEN TECHNOLOGY FOR NATURAL GAS SWEETENING USING NOVEL STATIC SYSTEM

Julia da Costa Moraes<sup>a</sup>, Fabio Roselet<sup>b</sup>, Leonardo Moreira dos Santos<sup>a</sup>, Bárbara Polesso<sup>a</sup> and Sandra Einloft<sup>a,\*</sup>

<sup>a</sup>Programa de Pós Graduação em Engenharia e Tecnologia de Materiais (PGETEMA), Escola Politécnica, Pontifícia Universidade Católica do Rio Grande do Sul, 90619-900 Porto Alegre – RS, Brasil

<sup>b</sup>Departamento de Oceanografia, Universidade Federal de Rio Grande, 96203-900 Rio Grande – RS, Brasil

Received: 09/22/2023; accepted: 01/24/2024; published online: 03/20/2024

Photosynthetic microorganisms have been widely studied as an alternative technology for CO<sub>2</sub> capture. Aiming to overcome some operational challenges in the application of these microorganisms for gas treatment on a large scale, the immobilization of microalgae in solid matrices emerges as an alternative to facilitate effective management of microalgae culture during harvesting process. In this work, different matrices for microalgae immobilization composed of silica/alginate were obtained varying silica precursors. The synthesized materials were characterized in terms of their specific surface area, cell viability, transparency and physical-chemical properties. Additionally, a new methodology was developed to evaluate the CO<sub>2</sub> capture by microalgae using a pressurized system with natural gas mixture. Tests were carried out exploring the influence of some variables, such as headspace volume, cell concentration, stirring and pressure. Once the optimized parameters were established, the amount of CO<sub>2</sub> captured by immobilized microalgae was investigated for 7 days by determining the CO<sub>2</sub> relative concentrations using gas chromatography. The results of immobilized microalgae showed levels of CO<sub>2</sub> removal of 41.4%. This work proved the potential application of the studied biomaterial for natural gas processing, making even more feasible the adoption of this technology for selective capture of CO<sub>2</sub> on an industrial scale.

Keywords: microalgae; carbon capture; silica hydrogel; immobilized microorganisms.

### INTRODUCTION

The increasing global demand for energy, added to the current and worrying environmental scenario, urgently drives the search for new technologies that guarantee a more sustainable economic and social development. To mitigate the harmful effects caused by the unbridled emission of harmful gases, industries everywhere are opting for cleaner energy matrices. Due to this fact, the increasing adoption of natural gas as a primary energy source has become more prevalent. According to the International Energy Agency (IEA), natural gas presently accounts for 23% of global energy demand, experiencing the most significant growth in consumption among all fuels during the past decade. As the interest in natural gas continues to surge, there is a growing imperative to advance technologies and innovations that optimize its processing. This development is crucial in reducing production costs and thus promoting the adoption of natural gas as an energy source. This energy sector generates hundreds of billions of dollars a year in economic activity and is expected to maintain rapid growth in the years ahead.<sup>1</sup> Currently, substantial investments are being made each year in the field of carbon capture. This is primarily due to the imperative of separating CO<sub>2</sub> from the natural gas stream, as required by legislation, to ensure both its energy value and industrial safety. Broadly speaking, there are three primary methods for capturing CO<sub>2</sub> from the gas mixture: absorption using chemical solvents (such as aqueous amine solution), adsorption through solid solvents, and membrane separation (selective polymeric barrier). Each technology is at a different stage of development and possesses its own limitations and drawbacks, including high energy expenditure, generation of toxic by-products, high production cost, low durability, etc.<sup>2</sup>

The use of gaseous waste to produce compounds of interest is an economically sustainable and attractive approach. In this context, microalgae, which are unicellular microorganisms, can represent

a great technological advance in the field of carbon capture and utilization,<sup>3</sup> once these microorganisms are capable of fixing CO<sub>2</sub> during photosynthesis while accumulating biomass, rich in proteins and lipids.<sup>4,5</sup> High CO<sub>2</sub> capture rates can be reached under ideal conditions,<sup>6</sup> as well as good tolerance to gas mixtures and selective CO<sub>2</sub> capture.<sup>7-9</sup> In 1993, Conde *et al.*<sup>10</sup> reported, for the first time, biogas purification using microalgae cultures, improving methane content in the gaseous flux. Although the potential of microalgae for methane gas processing has been already proven in the literature,<sup>11,12</sup> there are still a few studies exploring the applicability of microalgae for carbon selective capture processes in natural gas.<sup>13</sup>

The immobilization of microalgae in solid matrices emerges as an important strategy, offering substantial advancements in the feasibility of applying these microorganisms on a large industrial scale. This approach represents a significant operational optimization in the process of CO<sub>2</sub> biocapture. Unlike traditional cultivation, where the cells are free in the aqueous medium, the immobilization of microorganisms refers to the microalgae entrapment into a solid matrix, making their handling much more practical, overcoming a big economical challenge for the applicability of this technology in an industrial scale during the harvesting stage, which can actually represent 20-30% of the final cost of the process.<sup>14</sup> In addition, the use of this technique can avoid genetic mutations, ensure high cell density and increase cell tolerance to environmental factors, such as pH changes and temperature.<sup>15</sup>

Several parameters must be considered when choosing the material for the immobilization matrix, such as cytotoxicity and genotoxicity, chemical composition, synthesis method, surface morphology, mechanical and chemical stability, and, in the case of photosynthetic organisms, transparency.<sup>16</sup> Natural polymers (mainly alginates and carrageenan) are already well-consolidated materials for cell immobilization, being widely used for microorganisms entrapment.<sup>17</sup> Despite their high biocompatibility, their durability is limited due to their low stability in aqueous medium,<sup>18</sup> being susceptible to cell leakage. In addition, they exhibit low mechanical

\*e-mail: einloft@pucrs.br

resistance, high fracture susceptibility due to osmotic pressure of external conditions, and low-temperature stability.<sup>19,20</sup> As an alternative, silica materials are winning great credibility in the microorganisms entrapment context.<sup>21</sup> The use of silica as an immobilization matrix for microalgae has been studied mainly in the biosensors and metabolites production area.<sup>22-25</sup> Even though silica showed great results in previous studies, the inorganic matrix itself is still not completely ideal due to its rigid network, toxicity in certain concentrations, and high susceptibility to fractures.<sup>26</sup> Trying to overcome both limitations and combine characteristics of interest, hybrid materials appear as an attractive alternative.

There are still relatively few studies reported in the literature exploring the applicability of hybrid materials, associating viscoelastic biopolymers with resistant silica networks. In 1988, Fukushima *et al.*<sup>27</sup> described hybrid capsules with desirable properties using a simple and fast synthesis process. Since then, a few other attempts to obtain hybrid biopolymers using alginate and silica for cell immobilization were reported. Desmet *et al.*<sup>28</sup> explored a series of material optimizations by developing, for the first time, microalgae hybrid capsules for the production of high-value compounds. Nevertheless, the utilization of these hybrid capsules for CO<sub>2</sub> capture has never been explored thus far. This study aims to tailor a biomaterial consisting of microalgae immobilized in various hybrid matrices based on silica and alginate in order to obtain a system with intended purpose of CO<sub>2</sub> capture from natural gas and easy harvesting process of microalgae from the culture medium. The capacity of this biomaterial to capture CO<sub>2</sub> in a typical Brazilian pre-salt natural gas mixture (comprising 35% CO<sub>2</sub> and 65% CH<sub>4</sub>) is experimentally assessed. Furthermore, a novel methodology was developed to evaluate CO<sub>2</sub> capture by microalgae employing an innovative static system pressurized with simulate natural gas mixture.

## EXPERIMENTAL

### Microorganisms

The microalgae *Chlorella vulgaris* was chosen due to its large use in studies for CO<sub>2</sub> capture. The microalgae culture was maintained in Guillard *f/2* medium (marine water enhancement solution, Sigma Aldrich, 50× stock solution) at 25 °C under magnetic stirring for 24 h photoperiod using 40 W fluorescent lamps located 15 cm from the culture flask. The necessary volume of microalgae culture to be used in the CO<sub>2</sub> capture tests was estimated by direct counting in an optical microscope using a counting chamber.

### Synthesis of matrices for encapsulation

Two different silica precursors were investigated, individually or in combination, as a matrix material, with alginate. The synthesis of the matrix for encapsulation was based on the protocol presented by Fukushima *et al.*<sup>27</sup> and Desmet *et al.*,<sup>28</sup> which describe the formation of silica-alginate spheres through the dripping of the mixture of precursors in a solution of catalysts. The composition of each tested matrix is summarized in Table 1.

For the synthesis of matrix named A, sodium silicate (10× dilution,

25.5-28.5%, Sigma-Aldrich) solution was acidified until reached pH 8 using HCl 3 M. After pH adjustment, the silica solution was mixed with sodium alginate (3 wt.%, Sigma-Aldrich) in equal volumes. The mixture of silica-alginate was dropped in the catalyst solution (containing 0.4 wt.% poly(diallyldimethylammonium chloride) (PDADMAC) and 20 mM of CaCl<sub>2</sub>) under agitation, forming visible spheres. After 20 min, the capsules were washed in distillate water and left to mature in Guillard *f/2* culture medium for further tests. Matrix B was prepared analogous to matrix A, but the silica precursor used was colloidal silica (Ludox 40-HS, 2× dilution, Sigma-Aldrich) and the pH was adjusted to 7. For matrix C, the combination of the two silica precursors was explored (Ludox HS-40, 2× dilution and sodium silicate, 10× dilution). The silica solution was made by mixing the two precursors in 1:1 (v/v) proportion. Then, the pH was adjusted to 7 and the solution was mixed with sodium alginate in equal volumes. The synthesis followed the same steps as previously described. Table 1 summarizes the matrices synthesized for microalgae encapsulation. The main synthesis steps of the spheres and immobilization of microalgae are illustrated in the scheme shown in Figure 1.

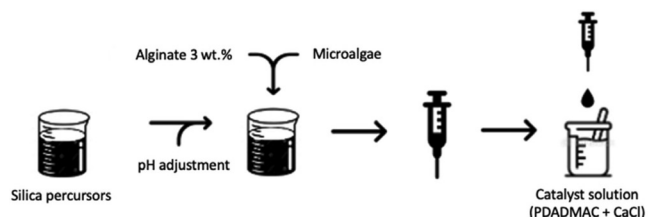


**Figure 1.** Scheme of synthesis steps for spheres obtaining and immobilization of microalgae

### Material characterization

The morphological characteristics of the hybrid beads surface were analyzed by field emission scanning electron microscopy (FE-SEM). The images were obtained using Inspect model F50 (FEI Company, Hillsboro, USA) microscope in secondary electrons mode. Samples were first dehydrated with successive ethanol baths of increasing concentrations followed by supercritical CO<sub>2</sub> drying. After that, the samples were coated with gold to become conductor and avoid any possible charging effects caused by the electron beam. Information on microalgae immobilization was obtained by analyzing the spheres in cross-sections.

The optical properties of the produced capsules were qualitatively evaluated using a stereomicroscope STEMI 305 model (Zeiss, Oberkochen, Germany). Images of the external layers of the material were obtained using Olympus PMG 3 reflection microscope and Image J software<sup>29</sup> was used to calculate the average diameter of spheres.

Fourier transform infrared spectroscopy (FTIR) was used to evaluate the functional groups present in the different matrices. For FTIR analysis, a spectrometer Spectrum 100 (Perkin-Elmer, Waltham, Massachusetts, USA) was used in UATR (universal attenuated total reflectance) mode. The range of recorded wavelengths was 4000 to 650 cm<sup>-1</sup> with a resolution of 4 cm<sup>-1</sup>.

The matrices specific surface area, specific pore volume and

**Table 1.** Composition (in proportions) of matrices synthesized for microalgae encapsulation

	Alginate / g	Coloidal silica (Ludox) / mL	Sodium silicate (HS-40) / mL
Matrix A: silicate/alginate	1	0	1
Matrix B: coloidal silica/alginate	1	1	0
Matrix C: silicate/ coloidal silica /alginate	2	1	1

mean pore diameter were evaluated using a Nova 4200 high-speed nitrogen adsorption surface area analyzer (Quantachrome, Boyton Beach, USA) and the analysis temperature was set to  $-196\text{ }^{\circ}\text{C}$ . The specific surface area was calculated using the BET equations (Brunauer-Emmett-Teller) and the average pore size was confirmed by the BJH method (Barrett-Joyner-Halenda).

The optical properties, FTIR and surface area analysis were carried out using spheres without microalgae. After synthesis, the spheres were dried at room temperature and atmospheric pressure for 2 days. Then, the spheres were kept at  $60\text{ }^{\circ}\text{C}$  for additional 24 h to ensure complete drying.

The autofluorescence property of photosynthetic pigments contained in microalgae was explored to identify the cell viability and distribution of microalgae in the capsules. For this purpose, a small transversal slice of the sphere was cut manually with the aid of a blade and immediately analyzed in a confocal fluorescence microscope model TCS SP8 (Leica, Wetzlar, Germany), using an excitation wavelength of 488 nm. The fluorescence signal was read in the 690-730 nm wavelength range. Cell viability was qualitatively assessed using apparent fluorescence intensity every 7 days, for 14 days, to obtain information about the functional durability of the biomaterial. During this period, the spheres containing the immobilized cells were maintained at same culture temperature and photoperiod conditions, without stirring.

### Immobilization of microorganisms

The cells were prepared by centrifuging a predetermined volume of microalgae culture (estimated by direct counting in the counting chamber) and resuspending the pellets in the sodium alginate solution (3 wt.%, Sigma-Aldrich). The cell entrapment was made following the same steps as matrix synthesis (previously described in sub-section Synthesis of matrices for encapsulation), with sodium alginate solution containing the microalgae cells.

### Bioreactor parameters optimization for $\text{CO}_2$ capture test

Aiming to overcome the complexity and related costs of traditional gas flow capture tests, this work proposes an alternative method based on a static pressurized system. The experimental apparatus is shown in Figure 2. A laboratory-scale bioreactor with a capacity of 200 mL, pressurized with a mixture of natural gas composed of 35%  $\text{CO}_2$  and 65%  $\text{CH}_4$  (Air Products, purity > 99.9%), was used. For optimization tests, the free microalgae culture was centrifugated, resuspended in Guillard f/2 culture media, added to the bioreactor, and the atmosphere air was purged through 5 cycles of natural gas mixture pressurization followed by depressurization, lasting 30 s each. The bioreactor was kept under the same conditions of temperature and photoperiod as the cell culture. Gas samples of  $30\text{ }\mu\text{L}$  were taken using a micro syringe and the relative concentration of the gases was analyzed by gas chromatography in day 0 and day 8.

Several optimization tests were carried out to determine the ideal parameters for the  $\text{CO}_2$  capture assay. The influence of headspace volume, cell concentration, stirring, and pressure on the system

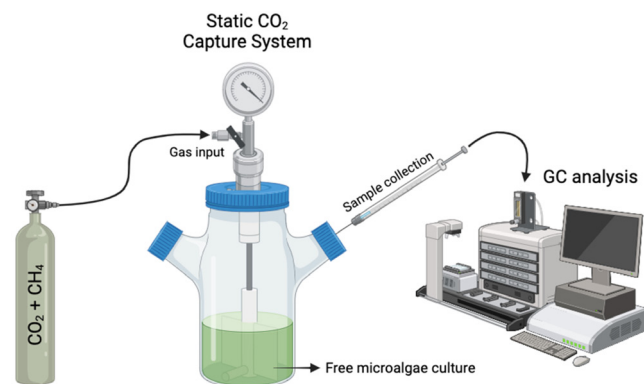


**Figure 2.** Scheme of experimental apparatus used for  $\text{CO}_2$  capture test using free microalgae

efficiency was explored. The parameters of study were chosen based on previous studies.<sup>30-32</sup> The conditions in which each variable was tested are shown in Table 2.

The influence of stirring was performed by filling 50% of the bioreactor capacity (100 mL) with  $10^6$  cells  $\text{mL}^{-1}$  density microalgae culture. The system was pressurized to 2 bar using natural gas mixture and the percentage of captured  $\text{CO}_2$  was evaluated. Continuous stirring (using a magnetic stirrer) and manual stirring (once *per day*) were tested. For comparison purposes, the gas concentration values in the absence of microalgae, using only the culture medium, were also measured.

After determining the influence of stirring, two cell densities were tested:  $10^6$  and  $10^7$  cells  $\text{mL}^{-1}$ , to investigate the effect of cell concentration on  $\text{CO}_2$  capture efficiency. In this test, 50% of the occupied bioreactor volume (100 mL of culture) was used and the system pressure was changed to 1 bar. The test was done with continuous magnetic stirring.

Tests were performed to determine if the amount of gas interferes with the ability to capture  $\text{CO}_2$  by microalgae in this system. For this, the headspace volume of the bioreactor was reduced to 10% and the pressure was changed to 0.7 bar. This test was done using  $10^7$  cells  $\text{mL}^{-1}$  cell density and with continuous magnetic stirring.

To make sure that the  $\text{CO}_2$  removal rate is due to microalgae biocapture, a test was run in presence of 10 mL silica matrix and pure culture media (until complete 180 mL) was used. The bioreactor was pressurized until 0.7 bar.

The optimized parameters were established once a satisfactory  $\text{CO}_2$  removal value was reached ( $\sim 30\%$ ).

### $\text{CO}_2$ capture test using immobilized microalgae

Once the parameters were established by previous tests (see sub-section Bioreactor parameters optimization for  $\text{CO}_2$  capture test), the  $\text{CO}_2$  biofixation by immobilized microalgae was finally investigated. The relative concentration of  $\text{CO}_2/\text{CH}_4$  was determined by taking samples once a day, for 8 days. The matrix that showed qualitatively the best results in terms of transparency, superficial area, and cell vitality was selected for this test.

**Table 2.** Optimization  $\text{CO}_2$  capture tests conditions

	Stirring	Cell concentration / (cells $\text{mL}^{-1}$ )	Headspace volume / mL	Pressure / bar
Test 1 (presence of stirring)	continuous or manually (1 <i>per day</i> )	$10^6$	100	2
Test 2 (cell density)	continuous	$10^6$ or $10^7$	100	1
Test 3 (headspace volume)	continuous	$10^7$	100 or 20	0.7
Test 4 (silica matrix)	continuous	-	20	0.7

The bioreactor was filled with 10 mL of spheres containing the immobilized microalgae and completed until 180 mL with culture medium. The test was performed using  $10^6$  cells  $\text{mL}^{-1}$ , 0.7 bar and under continuous magnetic stirring. The temperature and photoperiod were maintained as the same as culture conditions. The relative concentration of the gases was analyzed by gas chromatography for 8 days. To ensure that the measured  $\text{CO}_2$  captured is due to carbon biofixation by microalgae, another test was performed in the absence of microorganisms, using only the silica/alginate matrix and culture medium.

### Gas chromatography

The relative composition of the gas in the  $\text{CO}_2$  capture tests was determined by gas chromatography using a GC2014, Shimadzu equipment (Kyoto, Japan) coupled to a thermal conductivity detector (DCT). A Restek® CG capillary column (SchinCarbon ST 100/120; 2 m; 1 mm ID) was employed ( $140^\circ\text{C}$ ) and helium was used as carrier gas ( $10\text{ mL min}^{-1}$  flow). The natural gas mixture (relative  $\text{CH}_4$  and  $\text{CO}_2$  content) and the percentage of captured  $\text{CO}_2$  were evaluated. The  $\text{CO}_2$  captured by immobilized microalgae was calculated according to Equation 1:

$$\% \text{CO}_2 \text{ removal} = \frac{\% \text{CO}_2 \text{ initial} - \% \text{CO}_2 \text{ final}}{\% \text{CO}_2 \text{ initial}} \times 100 \quad (1)$$

## RESULTS AND DISCUSSION

### Physical and morphological proprieties of synthesized spheres

Since the  $\text{CO}_2$  capture potential by microalgae is closely tied to photosynthetic activity, it is important to ensure that the sphere matrix enables light to pass through. The transparency of matrices was qualitatively assessed by optical microscopy. The images of the spheres synthesized using different precursors are shown in Figure 3. The matrix B, composed by Ludox/alginate (Figure 3b),

was the one that exhibited qualitatively the highest transparency, while the silicate/alginate and silicate/Ludox/alginate matrices present a certain level of opacity, but still considered transparent (see Figures 3a and 3c). It is known that the optical properties of silica matrices are directly affected by the pH at which condensation is induced, changing the charges of the precursors and, consequently, the material morphology. The pH affects the interactions between particles, which can induce the formation of agglomerates and precipitates, causing light dispersion.<sup>33</sup> For better assessment of spheres transparency, future studies involving light transmittance analysis should be carried out.

The average diameter of the spheres varied based on the different matrices, as shown in Table 3.

This variation can be attributed to the presence of colloidal silica particles that hinder the condensation process of silane groups, limiting the contraction of the network. This phenomenon provides an explanation for the observed diameter variation. Also, the pH during condensation plays a significant role in the shrinkage of the silica network.<sup>34</sup>

The cross-sections images of the spheres, shown in Figure 4, confirm that the structure of all matrices consists of a rigid external layer and a core of viscous hybrid matrix of alginate/silica, as already described by other authors.<sup>28</sup> The literature also reports the presence of an extra external PDADMAC layer, which could be observed only in matrix B as shown in Figure 5, possibly due to its greater transparency. Further studies are needed to better understand the optical properties of hybrid silica/alginate materials.

SEM images shown in Figure 6 illustrate different morphologies of the capsules outer layer. The matrices containing colloidal silica particles exhibited a rough surface, probably due to the presence of colloidal silica particles, while the matrix composed only of silicate/alginate presented a smoother surface.

The spheres cross-sectional images (see Figure 7) evidence a tridimensional, porous and homogeneous morphology matrix. Furthermore, the presence of microalgae was observed in the core of the spheres, confirming microorganism's immobilization.

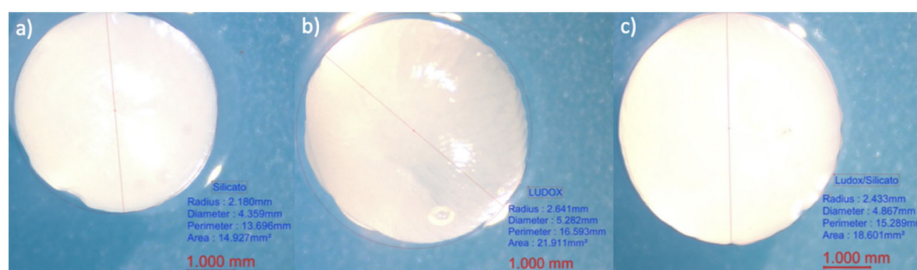


Figure 3. Optical microscopy images of the different spheres obtained: (a) silicate/alginate; (b) Ludox/alginate and (c) silicate/Ludox/alginate

Table 3. Average diameter, expressed in mm, of synthesized spheres using different silica precursors determined by optical microscopy

	Matrix A: silicate/alginate	Matrix B: Ludox/alginate	Matrix C: silicate/Ludox/alginate
Average diameter	$4.2 \pm 0.030$ mm	$5.15 \pm 0.098$ mm	$4.78 \pm 0.066$ mm

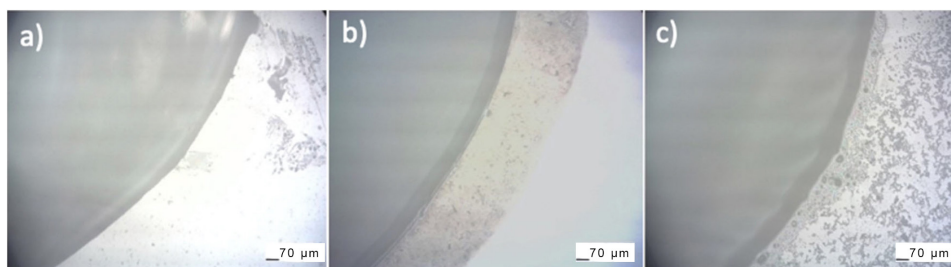
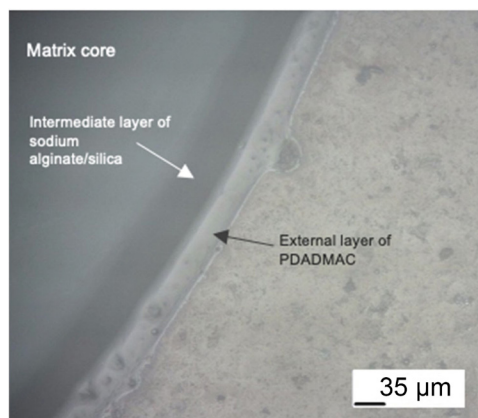


Figure 4. Optical microscopy image of spheres cross-sectional: (a) silicate/alginate; (b) Ludox/alginate; (c) silicate/Ludox/alginate



**Figure 5.** Optical microscopy image of cross-sectional slices of Matrix B (*Ludox/alginate*) sphere, highlighting the different outer layers

SEM images of matrix B and C (Figures 7b and 7c) reveal distinct granularity in the microalgae, suggesting the accumulation of silica nanoparticles on the cell walls of these microorganisms. Previous studies have documented the potential toxicity of nanosilica accumulation around cells on biological systems.<sup>35</sup> To investigate the impact of this particle deposition on cell viability, we further assessed the integrity of the photosynthetic system using fluorescence confocal microscopy.

### Surface properties of spheres

Considering the application of spheres as an encapsulating agent for microalgae to capture CO<sub>2</sub>, the diffusion of nutrients and other molecules (such as bicarbonate) is a key factor and is directly related to the porosity and specific surface area of the material.<sup>36</sup> The surface

characterization of materials according to their pore volume, surface area, porosity and pore distribution is fundamental for material selection and performance optimization for numerous industrial applications.<sup>37</sup> The adsorption and desorption curves of the different matrices are shown in Figure 8. According to Figure 8a, matrix A showed a typical type I (IUPAC classification) curve, being classic of microporous material. The steep adsorption uptake at low relative pressures is given by enhanced adsorbent-adsorptive interactions, and the limiting point is governed by the accessible micropore volume. When type I micropore isotherms do not reach a plateau below  $P/P_0$  values of approximately 0.1, it suggests that the sample may have a broader range of pore size distributions, including wider micropores and potentially narrow mesopores (< 2.5 nm). This classification aligns with type I (Figure 8b) isotherms, which is further supported by the average pore values documented in Table 4.<sup>38</sup> Hysteresis is a phenomenon commonly observed in porous materials, associated with the presence of metastable states, linked to capillary condensation of the molecular probe on mesopores. The low-pressure hysteresis observed in curve (Figure 8a) is commonly reported for some porous solids such as ordered mesoporous silicas and associated with the lack of equilibrium in the adsorption isotherm and/or the lack of proper outgassing, mainly found in porous materials where narrow pore constrictions are expected.<sup>39</sup> The isotherm of matrix B (Figure 8b) can be classified as a classic type IV, given by mesoporous adsorbents where the initial adsorption is followed by pore condensation at high relative pressure. After the pores are filled, the isotherm reaches a saturation plateau. When the capillary condensation is accompanied by the hysteresis phenomenon, as shown in Figure 8b, the curve is classified as type IV (a).<sup>40</sup> Finally, the isotherm of the biomaterial synthesized using a mixture of silica precursors (matrix C) can be classified by type V, showing weak adsorbent-adsorbate interactions at low relative pressure range. At high pressure, hysteresis took place,



**Figure 6.** SEM images of the spheres surface: (a) silicate/alginate; (b) *Ludox/alginate*; (c) silicate/*Ludox/alginate*

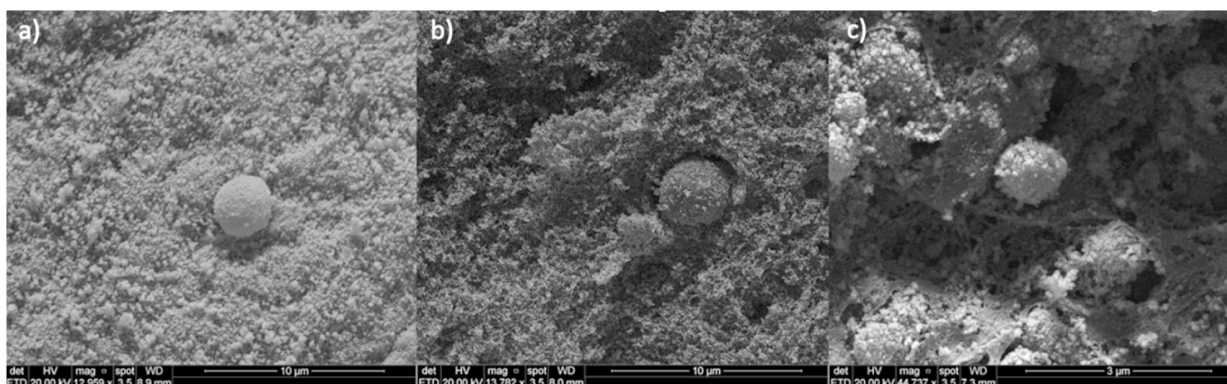


**Figure 7.** Spheres cross-section SEM images showing the presence of microalgae in the matrices: (a) silicate/alginate; (b) *Ludox/alginate*; (c) silicate/*Ludox/alginate*

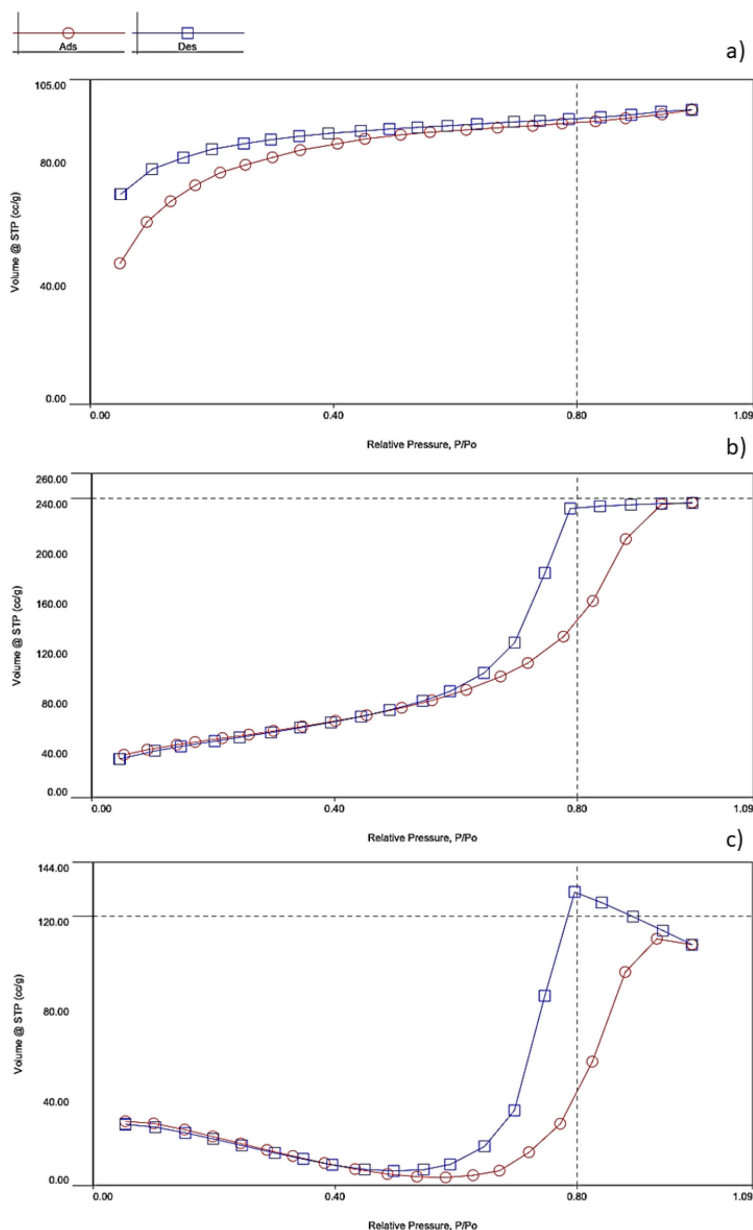


**Figure 8.** Adsorption (red) and desorption (blue) curves of the different matrices: (a) matrix A (silicate/alginate); (b) matrix B (Ludox/alginate); (c) matrix C (silicate/Ludox/alginate)

**Table 4.** Surface area, average pore volume and pore size for the different matrices

	Specific surface area / ( $\text{m}^2 \text{g}^{-1}$ )	Pore volume / ( $\text{cm}^3 \text{g}^{-1}$ )	Pore size / nm
Matrix A (silicate/alginate)	16.881	0.025	1.722
Matrix B (Ludox/alginate)	142.282	0.346	5.428
Matrix C (silicate/Ludox/alginate)	70.872	0.214	5.365

being analogous to type IV curves. Type V curves are also classic of mesoporous materials, confirming the data shown at Table 4.<sup>38,41</sup>

Specific surface area, average pore volume and pore size for the three different matrices are shown in Table 4. The composition of the sphere can drastically influence the textural properties, thus affecting the permeability of substances. It is noted that there is a greater similarity between the adsorption/desorption curves of matrix B (Ludox/alginate) and matrix C (silicate/Ludox/alginate), indicating that the presence of colloidal silica particles drastically influences the surface properties of the material. The specific surface area increased as the concentration of colloidal silica (Ludox) in the

material increased (Table 4). The synthesis of matrix C material likely leads to the formation of pores because it involves the condensation of soluble precursors (sodium silicate) around colloidal particles. These particles then act as a site for the formation of pores, which are surrounded by a silicate network. This suggests that increasing the concentration of colloidal particles leads to an increase in the material's porosity. According to Table 4, the presence of colloidal silica can also impact the pore size of the hybrid material network. The effect of colloidal silica particles in this kind of hybrid matrix has not yet been explored so far, and it would be beneficial to further investigate this phenomenon.

The matrix A, composed of silicate/alginate, showed a specific surface area of  $16.881 \text{ m}^2 \text{ g}^{-1}$ , while the specific surface area for the matrix C (silicate/Ludox/alginate) was about 4 times higher ( $70.872 \text{ m}^2 \text{ g}^{-1}$ ). The matrix B (Ludox/alginate) presented  $142.282 \text{ m}^2 \text{ g}^{-1}$  of surface area, showing higher porosity caused by the greater amount of colloidal silica particles.

The pore volume is also an important parameter for the diffusion of nutrients and gases in the material, being a critical point for cell survival and  $\text{CO}_2$  capture. High porosity and pore volume is also desired for obtaining metabolites of interest, such as lipids. According to Table 4, in all the matrices, the average pore volume varied into nanometric scale, which is smaller than the size of the microalgae (micrometric), ensuring the imprisonment of the cells in the matrix and preventing them from escaping into the medium and, simultaneously, ensuring proper nutrients and gas diffusion.

### Matrices molecular structure

The molecular structure, microstructure, morphology, optical and physicochemical properties of the capsules for microorganism immobilization directly depend on the polycondensation reactions during the sol-gel process, which in turn are directly affected by the nature of the silica precursors.<sup>42</sup> FTIR analyzes were carried out to determine the functional groups present in the different matrices. Figure 9 shows the characteristic bands of  $\text{COO}^-$  functional groups of alginate (at wavelengths  $1616$  and  $1421 \text{ cm}^{-1}$ )<sup>33</sup> present in all matrices. The bands at  $1062$  and  $789 \text{ cm}^{-1}$  correspond to the stretching of asymmetric and symmetric  $\text{Si-O-Si}$  bonds,<sup>43</sup> respectively, confirming the silica condensation. The peaks observed at  $972$  and  $943 \text{ cm}^{-1}$  represent  $\text{Si-OH}$  bonds,<sup>43</sup> indicating the presence of silane species generated during the hydrolysis step of the sol-gel process. The FTIR results confirm the similarity of the chemical composition of the three matrices, which is more evident in the case of matrix B (Ludox/alginate) and matrix C (silicate/Ludox/alginate). However, the small displacement of some characteristic bands and the relative signal decreasing observed for matrix C (silicate/Ludox/alginate) and matrix A (silicate/alginate) can indicate that the presence of sodium silicate can cause a change in the interaction of the compounds, probably due to the existence of  $\text{Na}^+$  ions. Nonetheless, it is important to emphasize that the concentration of the corresponding functional group has no direct relation to the intensity of the bands.

### Viability of immobilized microalgae in different matrices

The fluorescence of the photosynthetic pigments

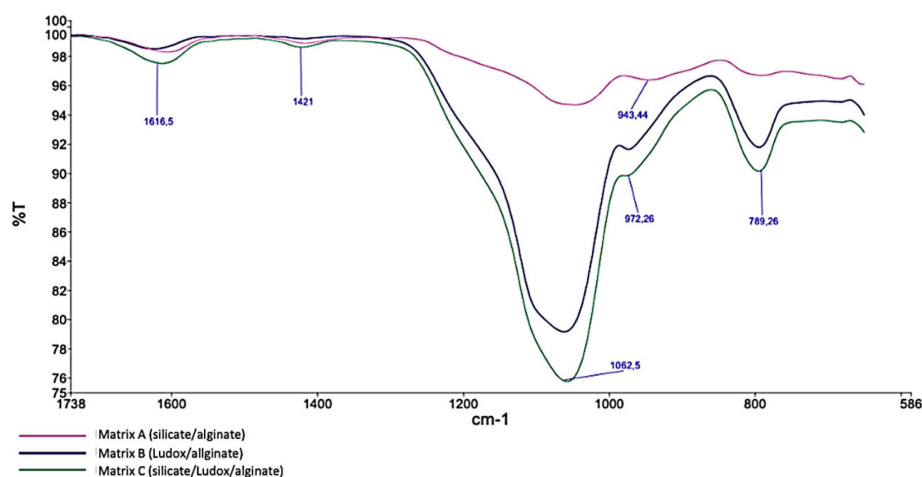


Figure 9. FTIR spectra for Ludox/alginate, silicate/alginate (zoom from  $586$  to  $1738 \text{ cm}^{-1}$ )

(chlorophyll a and b) was qualitatively evaluated by confocal microscopy to confirm the presence of microalgae inside the spheres and also to ensure that the photosynthetic apparatus remained intact after immobilization process. As can be seen in Figure 10, the presence of fluorescent spots in the nucleus of the spheres observed under confocal fluorescence microscope confirms that the cells were homogeneously distributed within the different hybrid matrices without affecting their photosynthetic apparatus during immobilization process. The durability of cell viability in different matrices was accessed by qualitatively analyzing, every 7 days, the presence and intensity of fluorescence points in the core of the spheres. After 7 days, the presence of cell clusters is observed (Figure 10), indicating that cell multiplication occurred. This result confirms that the microalgae maintained their ability to proliferate and cell clusters are formed because the solid matrix limits the mobility of these microorganisms. Cell multiplication in this type of hybrid matrix composed of silica/alginate has already been observed by other authors.<sup>44</sup> After 14 days, the spheres still showed some fluorescence when analyzed under microscope, but this light signal could not be detected by the digital images due to detector's resolution limit. This result demonstrates that, in this type of cultivation, the photosynthetic apparatus is maintained for approximately up to 14 days. It is important to comment that even if the conservation of the microalgae photosynthesis system was confirmed, indicating cell vitality, this result does not confirm its full functionality. For such confirmation,  $\text{CO}_2$  capture tests were performed.

### Results of the developed $\text{CO}_2$ capture system and influencing factors

A new design of a pressurized system was developed to study the capture of  $\text{CO}_2$  in batches. The influence of main parameters was first studied, such as stirring, cell concentration, headspace volume and pressure. These preliminary tests were performed with free microalgae aiming to determine the optimized conditions for further evaluating the  $\text{CO}_2$  capture by microalgae immobilized in alginate/silica spheres. The maximum  $\text{CO}_2$  captured as a function of agitation, cell concentration, pressure, headspace volume and presence of silica matrix is shown in Figure 11.

The results shown in Figure 11a confirm that constant agitation is essential for the process, helping the  $\text{CO}_2$  solubilization in the liquid medium and dissociation into  $\text{HCO}_3^-$  ions facilitating the cells accessing the ions and also maintaining cell suspension and right nutrient distribution. It is known that high levels of  $\text{CO}_2$  dissociation can cause acidification of the culture medium and consequently cell

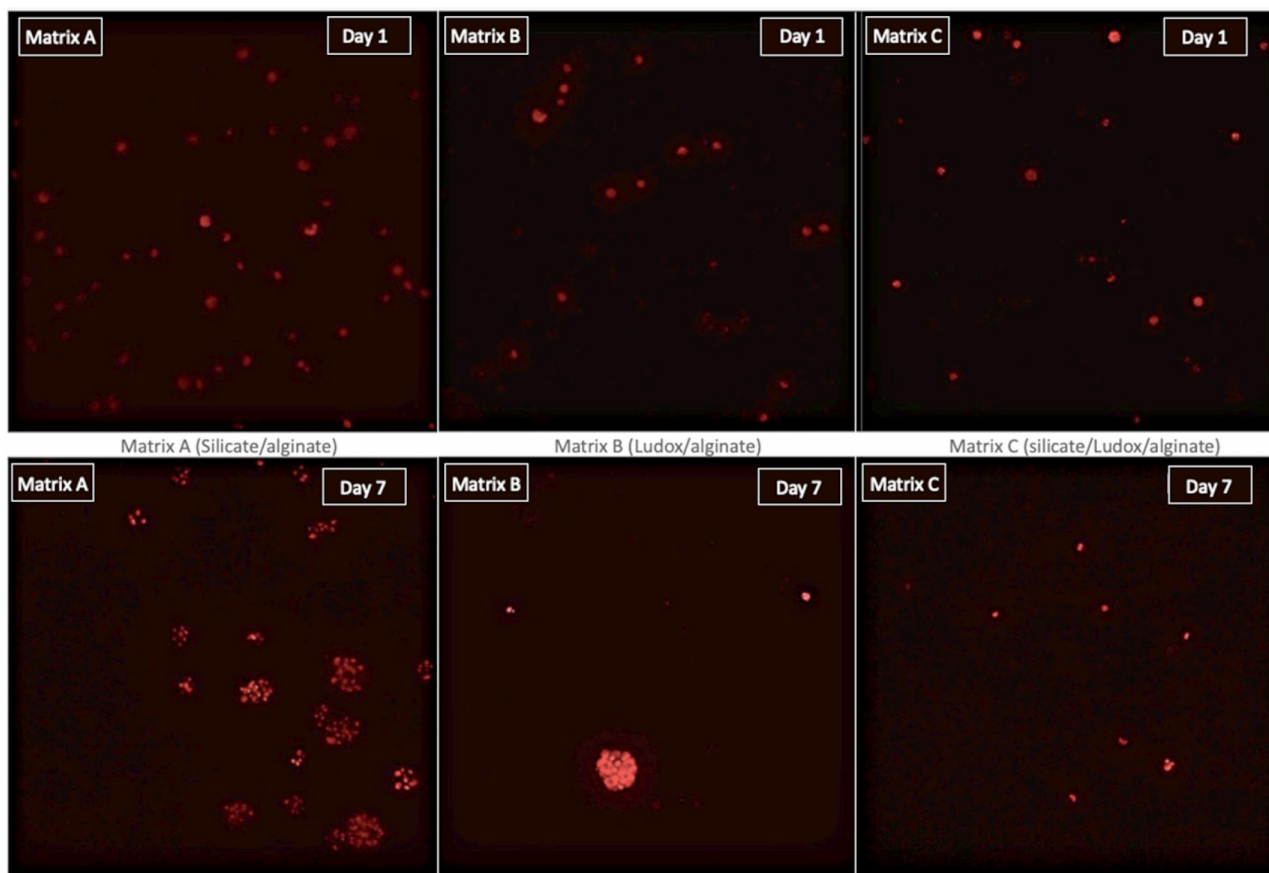


Figure 10. Image of confocal fluorescence microscopy of different matrices with immobilized microalgae (red) in day 1 and 7

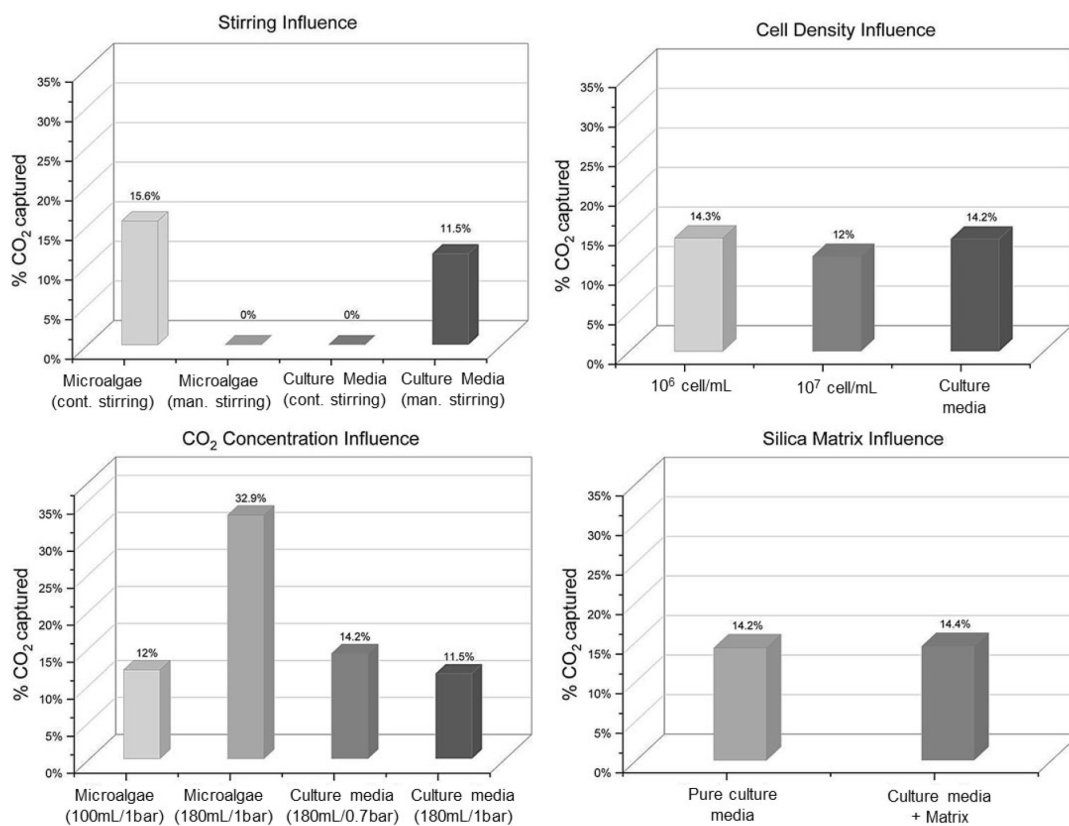


Figure 11. CO<sub>2</sub> removal as a function of (a) agitation, (b) cell density, (c) CO<sub>2</sub> concentration and (d) silica matrix

death, explaining why the levels of CO<sub>2</sub> captured by free microalgae was so close to that observed when using pure culture media. Aiming to minimize the toxic effect of low pH media, trying to achieve higher levels of %CO<sub>2</sub> removal, further tests were performed with a lower gas pressure (1.0 bar).

To evaluate the influence of cell density in captured CO<sub>2</sub>, two cell concentrations were tested: 10<sup>6</sup> and 10<sup>7</sup> cells mL<sup>-1</sup>. The capture results of both concentrations were similar (Figure 11b), indicating that the cell concentrations tested have no influence on CO<sub>2</sub> biofixation under tested conditions. However, it was found that the pH of the culture media decreased to 4 after 5 days, indicating that acidification media could be causing early cell death. It is important to mention that there is no report in literature indicating methane toxicity for microalgae. When reducing the volume of the reactor occupied by the gas (from 50 to 10%) and changing the system pressure to 0.7 bar, the CO<sub>2</sub> capture increased to 32.9% (Figure 11c), indicating that maybe high concentrations of CO<sub>2</sub> could be causing cell death. Based on these preliminary results, the best conditions found for CO<sub>2</sub> capture with microalgae to the next tests are 10<sup>6</sup> cells mL<sup>-1</sup>, 180 mL of cell culture media, 0.7 bar and magnetic stirring.

Moreover, to assess if the presence of silica matrix can interfere in the apparent CO<sub>2</sub> capture rate, more tests were run in presence of 10 mL of silica beads (matrix C was chosen for this purpose). The optimized parameters were used in this experiment. Relative CO<sub>2</sub> concentration was measured after 5 days. As can be noted in Figure 11d, the presence of the silica matrix does not influence the dissolution of the studied gas in the aqueous medium.

### Results of CO<sub>2</sub> removal by immobilized microalgae

Finally, the CO<sub>2</sub> removal potential by immobilized microalgae was evaluated using the developed pressurized system, with optimized parameters determined by previous tests, namely: cell concentration of 10<sup>6</sup> cells mL<sup>-1</sup>; pressure of 0.7 bar; 20 mL of headspace volume and magnetic continuous stirring. In the case of immobilized microalgae test, 10 mL of matrix was used, and the volume of the bioreactor was completed with culture media until reaching 180 mL.

The matrix chosen for this test was matrix C (composed of silicate/Ludox/alginate) due to its more suitable characteristics for the purpose of this work (determined by previous analysis). Figure 12 shows the percentage of CO<sub>2</sub> captured by microalgae cells immobilized in silica/alginate matrix for 7 days.

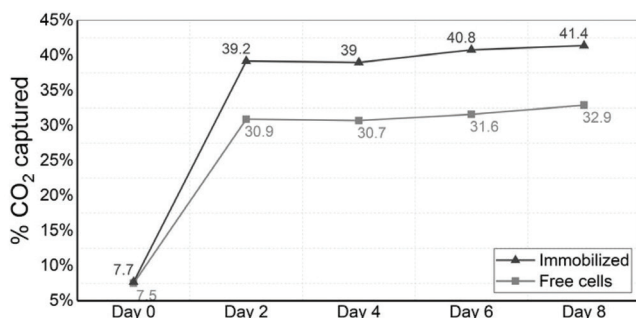


Figure 12. %CO<sub>2</sub> removal by immobilized and free microalgae

Although the obtained percentage of captured CO<sub>2</sub> in this study did not show as ideal numbers as already observed in the literature (60-90% removal),<sup>45-47</sup> such results should not be compared, since the adopted system in this work still lacks some optimizations and needs better understanding. Commonly, studies involving CO<sub>2</sub> capture tests by microalgae are carried out using gas flow systems. In Figure 12, it is possible to note that the CO<sub>2</sub> capture curve reaches a stationary

plateau after two days. This phenomenon probably occurs due to the previously mentioned toxic effect of CO<sub>2</sub>, indicating that although improvements in the process have been observed, the ideal conditions for CO<sub>2</sub> capture in this kind of system have only been partially achieved. However, due to some limitations of the used equipment, it was not possible to reduce gas concentration parameters. Even so, immobilized microalgae showed higher capture levels (41.4%) when compared to free microalgae (32.9%) (Figure 12), confirming the high potential applicability of this biomaterial for natural gas purification. Additionally, the results shown in Figure 12 also indicate a possible protective effect of the matrix on the immobilized cells, already documented in the literature,<sup>18</sup> evidenced by higher levels of capture when compared to free cells. Figure 13 summarizes the relative gas content of free and immobilized microalgae. It was possible to notice that no methane content was lost or absorbed by microalgae or culture media, and other volatile/gas products produced by microalgae during CO<sub>2</sub> biofixation were despicable.

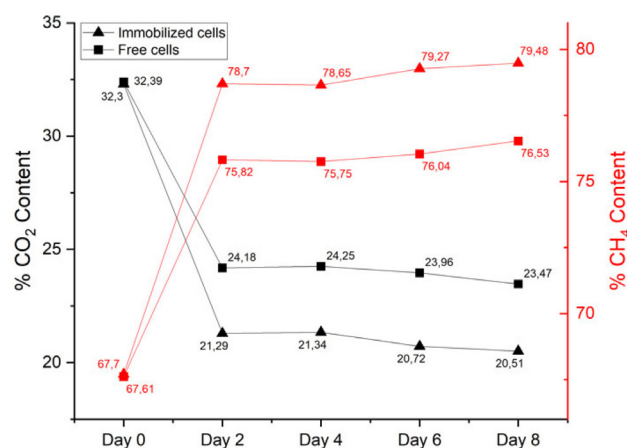


Figure 13. %CO<sub>2</sub> content (black line) and %CH<sub>4</sub> content (red line) of immobilized and free microalgae

### CONCLUSIONS

The present work aimed to develop optimized hybrid matrices (silica/alginate) for microalgae immobilization, by studying two different silica precursors and a combination of them. The materials were extensively characterized by their chemical composition, cell viability shelf life, optical proprieties and surface characteristics. It was observed that silica precursors have strong influence in the surface and porosity proprieties of synthesized biomaterials, although all materials showed a similar maintenance of cell viability and chemical composition. Additionally, a new pressurized system to study CO<sub>2</sub> uptake by microalgae was proposed, defining best system parameters by numerous tests in terms of presence of agitation, cell density, headspace volume and gas pressure. Finally, the matrix that showed more suitable characteristics (based on surface, optical and viability results) for the purpose of this work was selected and CO<sub>2</sub> capture tests was run using immobilized microalgae in matrix C. The results of immobilized microalgae showed levels of CO<sub>2</sub> removal even higher than those observed when using free microalgae (41.4 and 32.9%, respectively).

The aim of this study was to prove the significant potential of the developed biomaterial for natural gas processing, paving the way for further adoption of this alternative technology based on microalgae for CO<sub>2</sub> capture on an industrial scale, mainly facilitating the culture harvesting process. The findings described underscore the feasibility of selective CO<sub>2</sub> capture by immobilized microalgae on hybrid biopolymer/silica matrices, furthering the development of sustainable solutions.

Overall, this research contributes valuable insights to the field, providing a foundation for further advancements and applications of hybrid matrices for microalgae immobilization, specifically in the context of CO<sub>2</sub> capture. Yet, a deep understanding of biomass production could add economic value to the captured CO<sub>2</sub>.

## ACKNOWLEDGMENTS

S. E. thanks CNPq (316580/2021-0) for productivity research scholarship. J. M. thanks Hewlett-Packard (HP) for master scholarship.

## REFERENCES

- International Energy Agency; *Gas Market Report Q1 2023 including Gas Market Highlights 2022*, <https://www.iea.org/reports/gas-market-report-q1-2023>, accessed in February 2024
- Sifat, N. S.; Haseli, Y.; *Energies (Basel, Switz.)* **2019**, *12*, 4143. [Crossref]
- Onyeaka, H.; Miri, T.; Oibileke, K.; Hart, A.; Anumudu, C.; Al-Sharif, Z. T.; *Carbon Capture Sci. Technol.* **2021**, *1*, 100007. [Crossref]
- Sadvakasova, A. K.; Kossalbayev, B. D.; Bauenova, M. O.; Balouch, H.; Leong, Y. K.; Zayadan, B. K.; Huang, Z.; Alharby, H. F.; Tomo, T.; Chang, J. S.; *Algal Res.* **2023**, *72*, 103096. [Crossref]
- Jiang, L.; Luo, S.; Fan, X.; Yang, Z.; Guo, R.; *Appl. Energy* **2011**, *88*, 3336. [Crossref]
- Keffer, J. E.; Kleinheinz, G. T.; *J. Ind. Microbiol. Biotechnol.* **2002**, *29*, 275. [Crossref]
- Gebreslassie, B. H.; Waymire, R.; You, F.; *AIChE J.* **2013**, *59*, 1599. [Crossref]
- Kumar, A.; Yuan, X.; Sahu, A. K.; Dewulf, J.; Ergas, S. J.; Van Langenhove, H.; *J. Chem. Technol. Biotechnol.* **2010**, *85*, 387. [Crossref]
- Thomas, D. M.; Mechery, J.; Paulose, S. V.; *Environ. Sci. Pollut. Res.* **2016**, *23*, 16926. [Crossref]
- Conde, J. L.; Moro, L. E.; Travieso, L.; Sanchez, E. P.; Leiva, A.; Dupeiron, R.; Escobedo, R.; *Biotechnol. Lett.* **1993**, *15*, 317. [Crossref]
- Tongprawhan, W.; Srinuanpan, S.; Cheirsilp, B.; *Bioresour. Technol.* **2014**, *170*, 90. [Crossref]
- Srinuanpan, S.; Cheirsilp, B.; Kitcha, W.; Prasertsan, P.; *Renewable Energy* **2017**, *113*, 1229. [Crossref]
- Khoobkar, Z.; Amrei, H. D.; Heydarinasab, A.; Mirzaie, M. A. M.; *J. CO<sub>2</sub> Util.* **2022**, *64*, 102153. [Crossref]
- Molina Grima, E.; Belarbi, E. H.; Acién Fernández, F. G.; Robles Medina, A.; Chisti, Y.; *Biotechnol. Adv.* **2003**, *20*, 491. [Crossref]
- Wollmann, F.; Dietze, S.; Ackermann, J.; Bley, T.; Walther, T.; Steingroewer, J.; Krujatz, F.; *Eng. Life Sci.* **2019**, *19*, 860. [Crossref]
- Vasilieva, S. G.; Lobakova, E. S.; Lukyanov, A. A.; Solovchenko, A. E.; *Moscow Univ. Biol. Sci. Bull. (Engl. Transl.)* **2016**, *71*, 170. [Crossref]
- Gasperini, L.; Mano, J. F.; Reis, R. L.; *J. R. Soc., Interface* **2014**, *11*, 20140817. [Crossref]
- Moreno-Garrido, I.; *Bioresour. Technol.* **2008**, *99*, 3949. [Crossref]
- Mørch, Y. A.; Donati, I.; Strand, B. L.; Skjak-Braek, G.; *Biomacromolecules* **2006**, *7*, 1471. [Crossref]
- Hecht, H.; Srebnik, S.; *Biomacromolecules* **2016**, *17*, 2160. [Crossref]
- Lei, Q.; Guo, J.; Nouredine, A.; Wang, A.; Wuttke, S.; Brinker, C. J.; Zhu, W.; *Adv. Funct. Mater.* **2020**, *30*, 1909539. [Crossref]
- Peña-Vázquez, E.; Maneiro, E.; Pérez-Conde, C.; Moreno-Bondi, M. C.; Costas, E.; *Biosens. Bioelectron.* **2009**, *24*, 3538. [Crossref]
- Ferro, Y.; Perullini, M.; Jobbagy, M.; Bilmes, S. A.; Durrieu, C.; *Sensors* **2012**, *12*, 16879. [Crossref]
- Perullini, M.; Ferro, Y.; Durrieu, C.; Jobbagy, M.; Bilmes, S. A.; *J. Biotechnol.* **2014**, *179*, 65. [Crossref]
- Depagne, C.; Roux, C.; Coradin, T.; *Anal. Bioanal. Chem.* **2011**, *400*, 965. [Crossref]
- Meunier, C. F.; Dandoy, P.; Su, B. L.; *J. Colloid Interface Sci.* **2010**, *342*, 211. [Crossref]
- Fukushima, Y.; Okamura, K.; Imai, K.; Motai, H.; *Biotechnol. Bioeng.* **1988**, *32*, 584. [Crossref]
- Desmet, J.; Meunier, C. F.; Danloy, E. P.; Duprez, M. E.; Hantson, A. L.; Thomas, D.; Cambier, P.; Rooke, J. C.; Su, B. L.; *J. Mater. Chem. A.* **2014**, *2*, 20560. [Crossref]
- Schneider, C. A.; Rasband, W. S.; Eliceiri, K. W.; *Nature Methods* **2012**, *9*, 671. [Crossref]
- Polesso, B. B.; Bernard, F. L.; Ferrari, H. Z.; Duarte, E. A.; Vecchia, F. D.; Einloft, S.; *Heliyon* **2019**, *5*, e02183. [Crossref]
- Yan, C.; Zheng, Z.; *Appl. Energy* **2014**, *113*, 1008. [Crossref]
- Srinuanpan, S.; Cheirsilp, B.; Boonsawang, P.; Prasertsan, P.; *Bioresour. Technol.* **2019**, *281*, 149. [Crossref]
- Hernández-González, A. C.; Téllez-Jurado, L.; Rodríguez-Lorenzob, L. M.; *Carbohydr. Polym.* **2020**, *250*, 116877. [Crossref]
- Kurayama, F.; Suzuki, S.; Oyamada, T.; Furusawa, T.; Sato, M.; Suzuki, N.; *J. Colloid Interface Sci.* **2010**, *349*, 70. [Crossref]
- Mebert, A. M.; Baglolle, C. J.; Desimone, M. F.; Maysinger, D.; *Food Chem. Toxicol.* **2017**, *109*, 753. [Crossref]
- Perullini, M.; Amoura, M.; Roux, C.; Coradin, T.; Livage, J.; Japas, M. L.; Jobbágy, M.; Bilmes, S. A.; *J. Mater. Chem.* **2011**, *21*, 4546. [Crossref]
- Yang, X. Y.; Chen, L. H.; Li, Y.; Rooke, J. C.; Sanchez, C.; Su, B. L.; *Chem. Soc. Rev.* **2017**, *46*, 481. [Crossref]
- Kruk, M.; Jaroniec, M.; *Chem. Mater.* **2001**, *13*, 3169. [Crossref]
- Silvestre-Albero, A. M.; Juárez-Galán, J. M.; Silvestre-Albero, J.; Rodríguez-Reinoso, F.; *J. Phys. Chem. C* **2012**, *116*, 16652. [Crossref]
- Thommes, M.; Kaneko, K.; Neimark, A. V.; Olivier, J. P.; Rodríguez-Reinoso, F.; Rouquerol, J.; Sing, K. S. W.; *Pure Appl. Chem.* **2015**, *87*, 1051. [Crossref]
- Thommes, M.; *Chem. Ing. Tech.* **2010**, *82*, 1059. [Crossref]
- Innocenzi, P.; *The Sol-to-Gel Transition*, 2<sup>nd</sup> ed.; Springer: Cham, 2016. [Crossref]
- Wang, F.; Zhang, Z.; Yang, J.; Wang, L.; Lin, Y.; Wei, Y.; *Fuel* **2013**, *107*, 394. [Crossref]
- Pannier, A.; Soltmann, U.; Soltmann, B.; Altenburger, R.; Schmitt-Jansen, M.; *J. Mater. Chem. B* **2014**, *2*, 7896. [Crossref]
- Conde, J. L.; Moro, L. E.; Travieso, L.; Sanchez, E. P.; Leiva, A.; Dupeiron, R.; Escobedo, R.; *Biotechnol. Lett.* **1993**, *15*, 317. [Crossref]
- Kumar, A.; Ergas, S.; Yuan, X.; Sahu, A.; Zhang, Q.; Dewulf, J.; Malcata, F. X.; Van Langenhove, H.; *Trends Biotechnol.* **2010**, *28*, 371. [Crossref]
- Srinuanpan, S.; Cheirsilp, B.; Kitcha, W.; Prasertsan, P.; *Renewable Energy* **2017**, *113*, 1229. [Crossref]